

The degradation of oxadiazon by non-thermal plasma with a dielectric barrier configuration

Ying ZHAO (赵颖)^{1,2}, Risheng YAO (姚日升)², Yuedong MENG (孟月东)¹,
Jiaying LI (李家星)¹, Yiman JIANG (江贻满)¹ and Longwei CHEN (陈龙威)^{1,3}

¹Institute of Plasma Physics, Chinese Academy of Sciences, Hefei 230031, People's Republic of China

²School of Medical Engineering, Hefei University of Technology, Hefei 230009, People's Republic of China

E-mail: lwchen@ipp.ac.cn

Received 11 July 2016, revised 15 November 2016

Accepted for publication 20 November 2016

Published 21 February 2017



CrossMark

Abstract

To explore the feasibility of a degradation approach by non-thermal plasma and the corresponding degradation pathways, studies on the oxadiazon removal in synthetic wastewater by a dielectric barrier discharge plasma reactor were investigated. The loss of the nitro group, dechlorination and ring cleavage is mainly involved in the non-thermal plasma degradation pathways of oxadiazon in a solution based on the OES and LC-MS analysis. Detection of EC25 and the production of the chlorine ion and nitrate ion further demonstrate the feasibility and validity of the approach. The conditions with a proper applied voltage, solution flow rate, oxygen flow rate, and solution pH contribute to the plasma degradation processes with a degradation ratio of over 94%.

Keywords: oxadiazon, wastewater degradation, DBD non-thermal plasma

(Some figures may appear in colour only in the online journal)

1. Introduction

Wastewater with a high concentration of organics poses a threat to the aquatic environment and results in a short- and long-term impact on humans and ecosystems [1]. The increasing accumulation of persistent organic pollutants (POPs) in the environment are mainly from the widespread discharge of industrial wastewater effluent; and extensive production, consumption, and utilization of chemical products. These pollutants are known to be toxic and difficult to remove by conventional biotechnology, which was believed to be an efficient and economical method to treat organic wastewater [2]. Oxadiazon (molecular formula $C_{15}H_{18}C_{12}N_2O_3$), which belongs to the chlorinated organic compounds, is a pre-emergence and post-emergence herbicide used widely in many countries [3–6] to control weeds in

agricultural fields. The chemical structure of oxadiazon is illustrated in figure 1.

Several advanced oxidation processes (AOPs) have been developed, such as direct ozonation [7], ultrasonification [8], ultraviolet (UV) photolysis [9–11], Fenton process [12], TiO_2 -photocatalysis [13–15] and non-thermal plasmas [16–21] have been developed to dissociate the POPs. Mechanisms of the AOPs mainly attribute to the chemical active species, e.g. ozone, hydrogen peroxide, singlet oxygen, hydroxyl radical, and others. Among the active species, hydroxyl radical is nonselective, unstable and the most reactive with the highest oxidation potential of 2.33 V compared to O_3 , H_2O_2 , or $KMnO_4$ whose oxidation potentials are 2.07 V, 1.77 V, and 1.67 V, respectively [2, 22]. Currently, the main methods for degradation of oxadiazon include photo degradation (TiO_2 catalysis or sunlight), Fenton reagent, biodegradation, and some combinations of them [4, 13, 23–28]. Non-thermal plasma technologies which can generate these active species have many advantages, e.g. the non-addition of external

³ Author to whom any correspondence should be addressed.

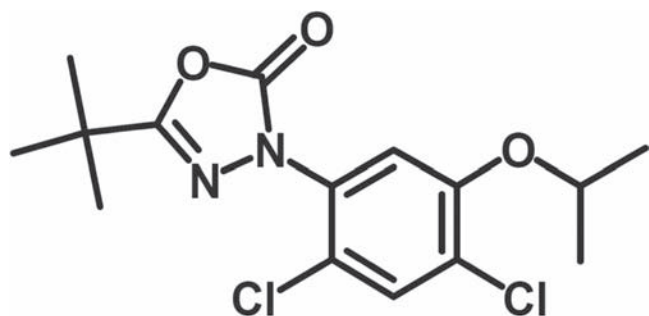


Figure 1. Chemical structure of oxadiazon.

chemicals, environmental compatibility, simplicity of operation at atmosphere, effectiveness, non-generation of secondary pollution, and the ability to kill bactericidal activity [29, 30]. M Magureanu *et al* [31] studied three blactam antibiotics (amoxicillin, oxacillin and ampicillin) in an aqueous solution utilizing a dielectric barrier discharge (DBD) with a coaxial configuration. After 60 min plasma treatment, a 92.5% removal of pentoxifylline was achieved. Yanan Liu *et al* [32] investigated the degradation of carbamazepine (CBZ) in the aqueous solution treated by DBD plasma. The result showed that 100% CBZ was removed after 3 min of treatment with the *ex situ* discharge. However, after 60 min with the *in situ* discharge, only about 81% was achieved. Kim *et al* [33] investigated the degradation of antibiotics in synthetically prepared wastewater by DBD plasma treatment. The effects of discharge power, initial concentration, working gas type (air or O₂) and working gas flow rate on the degradation were studied and discussed. Maria *et al* [34], for the first time, assessed for cyanide removal from the aqueous solutions at laboratory scale by two different non-thermal DBD plasma reactors (conventional batch reactor and coaxial thin falling water film reactor) at atmospheric pressure. After 3 min treatment with the coaxial thin falling water film reactor, more than 99% cyanide was removed. So far, we have not found the degradation of oxadiazon by a non-thermal plasma. And, therefore, the degradation pathway for plasma treatment still remains unknown. In this paper, we present a possible degradation mechanism on the oxadiazon degradation by the non-thermal plasma method.

This paper is organized as follows. In section 2, the experimental section including material and procedures, apparatus and methods, analysis and measurement will be described in detail. In section 3, the results including the effect of external parameters, e.g. discharge power, gas flow rate, solution flow rate, and the solution pH, on the oxadiazon degradation are presented. Furthermore, the possible degradation pathways are analyzed and discussed. Finally, a summary is given.

2. Experiment

2.1. Material and procedures

Analytically pure (AP) Oxadiazon (97.5%, powder) and guarantee reagent (GR) methanol (99.7%, liquid) were purchased from Aladdin (Shanghai, China). Sodium hydroxide

(AP) was provided by Sinopharm (Shang Hai, China). And the water used throughout this experiment is high performance liquid chromatography (HPLC) quality. Since the oxadiazon has low solubility in water, but is readily soluble in most organic solvents, the powder of oxadiazon with weight of 2 gram is first stirred and dissolved in 30 mL methanol which is vulnerable to oxidization into CO₂ and water by Ar/O₂ plasma in DBD reactor. Then the high-concentration oxadiazon solution was further dissolved into the oxadiazon density of 1200 mg·L⁻¹ with distilled water. Finally, a proper amount of the oxadiazon solution was taken and diluted with distilled water to prepare aqueous solutions of 10 mg·L⁻¹, 20 mg·L⁻¹, 40 mg·L⁻¹, and 80 mg·L⁻¹, respectively. The prepared solution with standard density was used not only as samples for the experiment, but also the standard solutions to draw a standard curve for liquid chromatography (LC) analysis. The testing reagents for COD A+B, nitrate, and chloride in solution were purchased from Merck (Germany). The COD solution A and B were in a large packing with a measuring range of 25–1500 mg·L⁻¹, which will be described in the latter section.

2.2. Apparatus and methods

The schematic diagram of the apparatus is shown in figure 2 which consists of a plasma reactor (DBD plasma reactor with coaxial configuration), gas supply system, water-cycling system, off-gas system, and measuring equipment. The discharge chamber was composed of an inner electrode, an outer electrode and a quartz tube which are about 1.5 mm in thickness. The gap between the inner electrode and the quartz tube is about 3 mm which allows the working gas and solution pass through. Considering of the electric conductivity of some treated solutions, the inner electrode which is directly in contact with the solution was connected to the ground. The solution was pumped from the water tank to the discharge chamber by a peristaltic pump (BT600-2J) with a certain flow rate ranging from 0.07–3000 mL min⁻¹. Solution enters into the discharge chamber from the entrance at the bottom of the inner electrode, and then drops along the outer surface of the inner electrode forming a water film from the top of the electrode. Finally, the solution returns back to the water tank forming a circulation system. Ar (99.99%) and O₂ (99.99%) controlled by two mass flow meters (D07-7B, Sevenstar[®]) were separately introduced into the discharge chamber. The plasma was generated in the gap between the water film and the quartz tube when the power source was applied on the electrodes. One procedure was carried out to prevent the atmosphere air from entering into the discharge chamber. The remaining air was replaced by the working gas, i.e. argon and oxygen, for about 5 min before plasma treatment. The schematic diagram and the photograph of the discharge were shown in figure 3. The high voltage (HV) probes and current connected directly to the electrode were used to collect the signals of voltage and current which were recorded by a digital oscilloscope (Tektronix, TDS-3012). A Canon digital camera with 50 ms exposure time was used to take the optical imaging of the discharge.

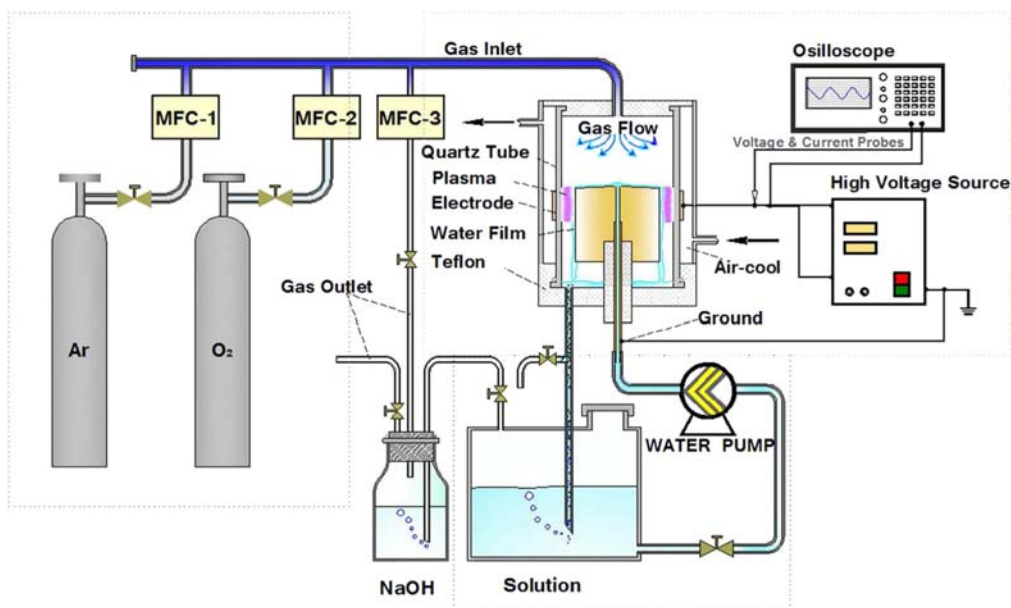


Figure 2. Schematic diagram of experimental setup.

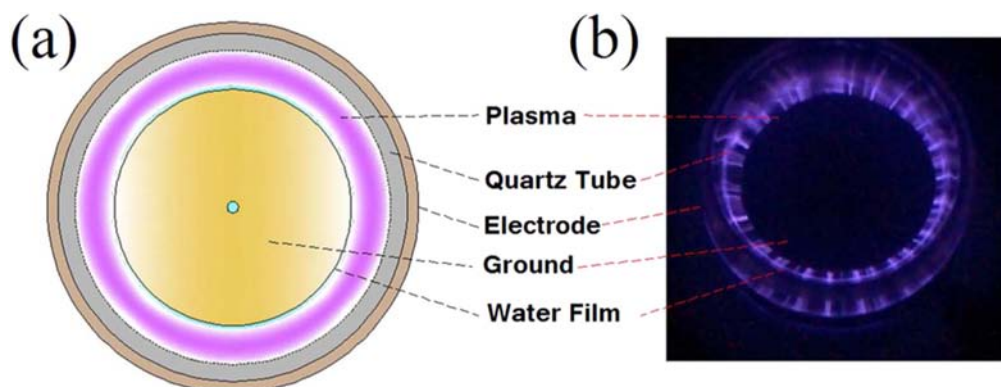


Figure 3. (a) The schematic diagram, and (b) the photograph of the coaxial plasma reactor.

Table 1. Experimental conditions.

No.	C_0 (mg · L ⁻¹)	Voltage (kV)	Solution Flow Rate (L · h ⁻¹)	O ₂ Flow Rate (mL · min ⁻¹)	pH
1#	40	6	9.6, 14.4, 19.2, 24.0	40	7
2#	20	4, 5, 6, 7.5	14.4	40	7
3#	20	6	14.4	10, 20, 40, 80	7
4#	10, 20, 80	6	14.4	40	7
5#	20	6	14.4	40	5, 7, 9, 12

In this work, the probable factors including the voltage of discharge, the O₂ flow rate, the solution flow rate, initial oxadiazon concentration, and the initial solution pH, were investigated. The experiment parameters were presented in table 1 where the argon flow rate was set into 40 mL min⁻¹. For comparison, the amount of synthetic oxadiazon solution was 60 mL, and the total plasma treatment time was ranging from 180 min to 300 min for different working conditions. Samples with volume of about 0.5 mL were collected every 5 min during the first half hour, then every 30 min in the remaining treatment.

2.3. Analyses and measurements

COD was a measure of the total quantity of oxygen required to oxidize all organic material into carbon dioxide and water. The UV/VIS spectrometer (PHOTOLAB-6100, Germany) was implemented to detect the COD of the samples. The measurement range was 25–1500 mg·L⁻¹. To approximately determine maximum absorption wavelength and observe the possible structural change of samples, the UV spectra ultra-violet spectrophotometry (UV2550, Shimadzu, Japan) was adopted. High performance liquid chromatography (HPLC,

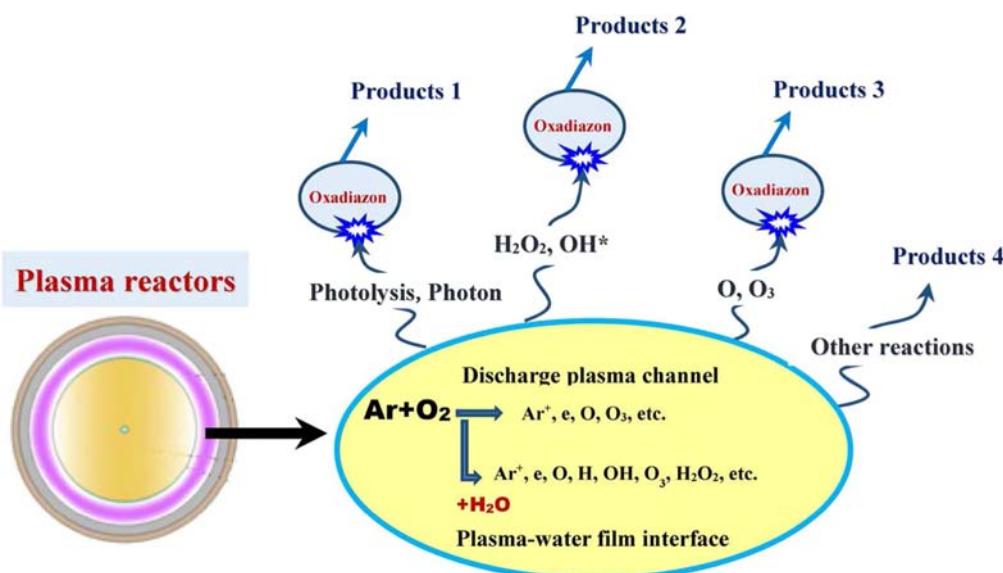


Figure 4. Oxidation processes inside the plasma channel.

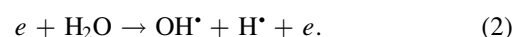
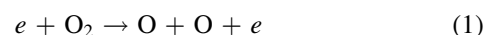
Agilent 1200) with a C18 ($5\ \mu\text{m}$, $4.6\ \text{mm ID} \times 150\ \text{mm}$) reversed-phase column was used to determine the contents of the oxadiazon in each sample in the first half hour. The mobile phase was methanol-water (80:20 in volume ratio) with the flow rate of $0.8\ \text{mL}\cdot\text{min}^{-1}$. The column temperature was set at 25 degrees. The oxadiazon concentration of each sample needed to be measured and calculated according to the relationship between the standard oxadiazon concentration and peak area mentioned previously. Then the removal rate of oxadiazon can be obtained. The nitrate test, nitrite test and chloride test could also be determined by Merck reagent and UV/VIS spectrometer. TOC, the pH, and the electrical conductivity of the samples were measured by TOC Analyzer (Multi N/C 2100, Germany), pH meter (PHS-3D, China), and conductivity meter (DDS-320, China), respectively. Optical Emission Spectroscopy (OES) was one of the principal methods for plasma diagnostics. The chemical active species of the generated plasma were diagnosed by OES (Avaspec-2048, Netherlands) with a Charge Coupled Device (CCD) camera and multichannel. The scanning wavelength ranges and the precision of the OES monochromator were 200–1160 nm and 0.1 nm respectively. Liquid chromatography-electrospray ionization tandem mass spectrometry (LC-ESI-MS/MS, LTQ Orbitrap, ThermoFisher) system equipped with a PLRP-S chromatographic column was employed to analyze the substances during the degradation process.

3. Results and discussion

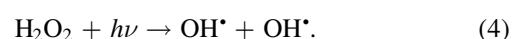
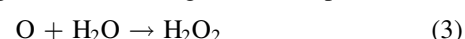
3.1. Optical emission spectrum analysis

Many studies of electrical discharges in the presence of water solution have been developed since Faraday's work in 1832. However, the inner mechanisms underlying in the degradation process still remain unknown. It is estimated that the electric discharge generates electrons and active atoms which

could dissociate water into hydroxyl and hydrogen radicals. Subsequent works further demonstrate the formation of hydrogen peroxide and hydroperoxyl which are easily dissolved in water and possess high oxidation [35]. Plasma formed on the surface of aqueous solutions dissociates water into highly oxidative and reductive radicals, which can induce chemical changes by oxidation and reduction processes in the compounds present in the solutions. Figure 4 shows the schematic oxidation processes in the plasma channel. As can be seen, various reactions occur on the plasma-water film interface to degrade oxadiazon solution. The main oxidative species generation reactions are described below. The electrons in the plasma generated at atmospheric pressure lost their energies due to strong, inelastic, and frequent collisions with heavy particles which initiate various processes including ionization, vibrational/rotational excitation and electron attachment. The processes result in the fact that it is hard to obtain large amount of electrons with high energy because the actual energy of electrons in plasma is a distribution over a wide range of energies and only a small percentage of the electrons in the high tail of the electrons energy distribution function have energies greater than the ionization and excitation potential. As a result, water molecules and oxygen can perform direct dissociation by electron impact



In the plasma water interface, atom oxygen contacts with water and converts into hydrogen peroxide. Photolysis of hydrogen peroxide is due primarily to the absorption of a different wavelength of ultraviolet generated in plasma



In addition to these primary species, an ozone with high concentrations was detected because of the various secondary reactions

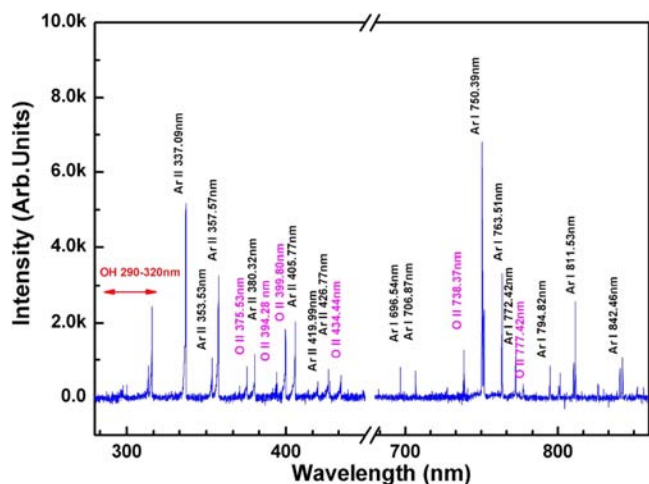


Figure 5. OES of the non-thermal DBD plasma on normal condition.

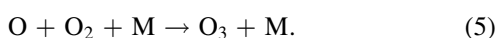


Figure 5 shows a typical optical emission spectrum (OES) of DBD plasma in the cases of water film. As can be observed, the main emission lines include $O^*(3d^4F^0 \rightarrow 3p^4D, 375.57 \text{ nm}; 4d^2F \rightarrow 3p^2D^0, 391.75 \text{ nm}, 394.29 \text{ nm}; 3p^1P \rightarrow 3s^1D^0, 399.80 \text{ nm}; 4f \rightarrow 3d^4D, 434.44 \text{ nm}; 4p^2F^0 \rightarrow 3d^2D, 738.37 \text{ nm}; 3p^5P \rightarrow 3s^5S^0, 777.42 \text{ nm})$, Ar ($4p \rightarrow 4s, 405.77 \text{ nm}, 696.54 \text{ nm}, 750.39 \text{ nm}, 763.51 \text{ nm}, 772.42 \text{ nm}, 794.82 \text{ nm}, 810.37 \text{ nm}, 811.53 \text{ nm}, 826.45 \text{ nm}, 842.46 \text{ nm}; 4d \rightarrow 4p, 337.09 \text{ nm}, 380.32 \text{ nm}; 5d \rightarrow 4p, 357.58 \text{ nm}; 4f \rightarrow 3d, 419.99 \text{ nm}; 5p \rightarrow 4s, 426.77 \text{ nm}; 6s \rightarrow 4p, 706.87 \text{ nm}; 3d \rightarrow 4p, 750.52 \text{ nm})$, and OH ($297\text{--}316 \text{ nm}$). Moreover, UV light and shock waves could also be generated depending on the solution conductivity and the intensity of the discharge energy during the electrical discharges in the presence of water [29]. In the weakly ionized plasmas primary and secondary molecular, ionic, and radical species generated by the discharge can attack the components contained in the solution and cause their degradation. The complicated aspects such as active species, UV light, shock wave, and charged particles result in the complexity of the degradation processes, which might generate many kinds of intermediate products.

3.2. Degradation processes and mechanisms for oxadiazon

3.2.1. Oxadiazon removal and TOC. Both parameters (COD and TOC), which directly evaluate the pollution level of an aqueous solution, are generally in a linear relation. From the toxicological point of view, the TOC analysis which takes into consideration all the residual carbon-containing metabolites, seems more accurate and appropriate for the decontamination of polluted waters containing organics. Figure 6 shows the removal rate of the oxadiazon and degradation of the TOC of the solution during the plasma treatment process. As can be noted, the removal rate of the oxadiazon increases in the plasma treatment time. The removal rate reached up to 94.8% after 1 min plasma treatment. Then it gradually increased further from 94.8% to about 98.96% after plasma degradation of 30 min. While

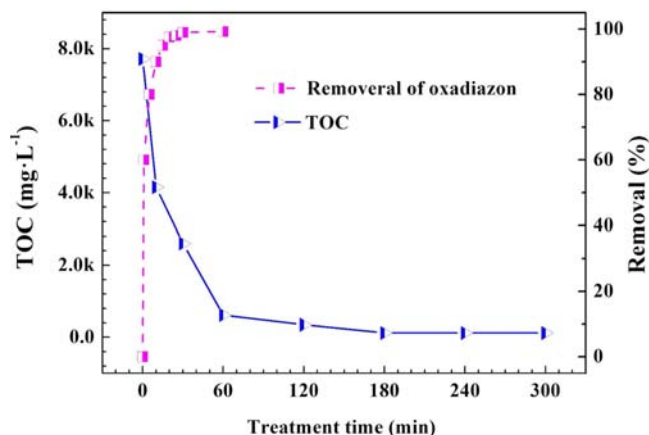


Figure 6. Variation of oxadiazon removal and TOC with treatment time.

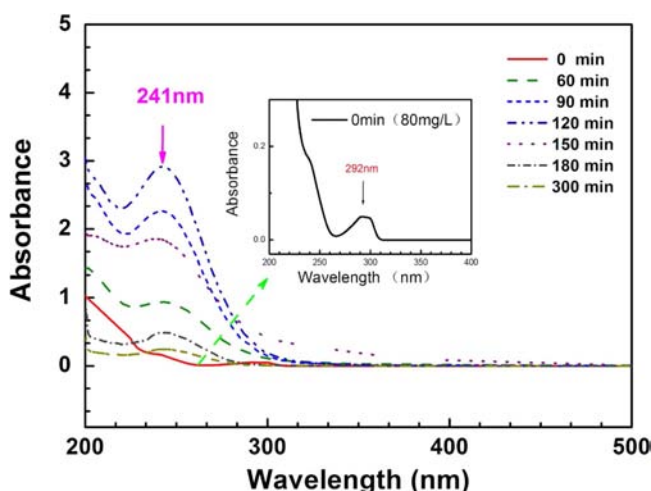


Figure 7. UV-visible spectra of the oxadiazon solution before and after plasma treatment.

the TOC decreased gradually with the non-thermal plasma treatment time, which implies that some components containing carbon produced by the degradation progress are consistently degraded into carbon dioxide and eliminated from solution in spite of the exhibition of the concentration of the total intermediate products. According to this, it seems more reasonable that there are two dominant processes co-existing in the plasma degradation process, i.e. the process decomposed components with large molecular weight into small fragments which resulted in the increase of the concentration of intermediate products, and the process oxidizing the fragments into carbon dioxide which results in the loss of carbon elements. The former plays a dominant role in the first stage of the plasma degradation process, and then the latter has a role in the later stage.

3.2.2. UV-visible spectra and analysis of NO_3^- and Cl^- .

Figure 7 shows the absorption spectra of the oxadiazon sample before and after plasma treatment. As can be viewed, the absorption spectra of the sample before plasma treatment was characterized by an absorption band in the wavelength ($\lambda_m = 292 \text{ nm}$) which is responsible for the original

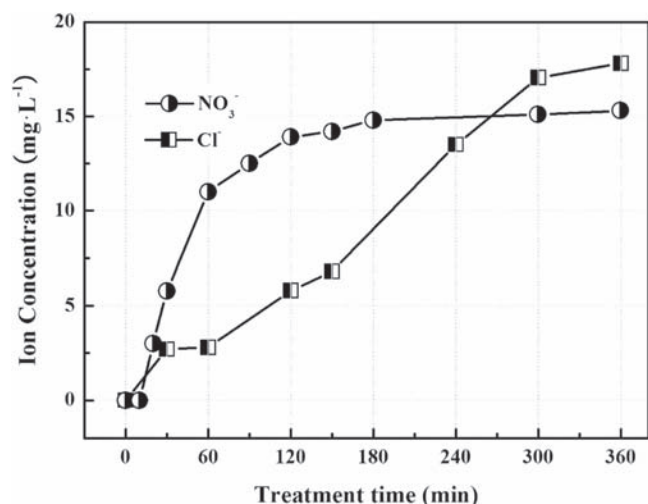


Figure 8. Variation of NO₃⁻ and Cl⁻ with plasma treatment time.

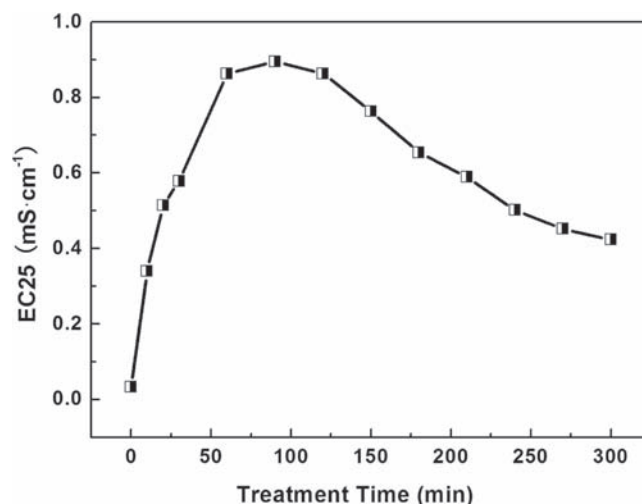


Figure 9. Variation of electric conductivity with plasma treatment time.

oxadiazon solution. However, the absorption spectra was shifted to the wavelength range ($\lambda_m = 241$ nm) after plasma treatment. Although it is not possible to identify the exact species contained in the solution sample, we can still learn that the components in the solution were altered from oxadiazon to some organics having the structure composed of 5- and 7-member rings characterized by the Woodward–Fieser rules [36–38]. The intensity of absorption spectra at 241 nm first increases and reaches its climax with the plasma treatment time ranging from 0 min to 150 min, then decreases for the plasma treatment time. According to the Lambert–Beer law, the total concentration of the multi-components performs the similar trend. The result might indicate that the oxadiazon with chemical formula C₁₅H₁₈C₁₂N₂O₃ gradually degrades into small fragments with plasma treatment.

The production of chloridion and nitrate ion happens along with the plasma degradation process. The evolution rule of them could reflect the plasma generation pathway to some extent. Variation of NO₃⁻ and Cl⁻ with plasma treatment time is presented in figure 8. It shows that chloridion and nitrate ion increase with the time. The time for nitrate ion to reach stability is much less than the one for the chloridion. And the increase rate of nitrate ion is faster than the chloridion, which would be due to the possible mechanism that some parts of nitrogen removal process are prior to the loss of chlorine atoms during the plasma degradation process.

3.2.3. Electric conductivity of the solution. As products such as chloride and nitrate are produced and dissolved in solution, the electric conductivity of the solution will be influenced. Figure 9 shows the variation of electric conductivity with the plasma treatment time. As can be observed, the electric conductivity (EC25) first increases to a maximum, then decreases with the plasma treatment time.

3.2.4. Degradation pathways for oxadiazon. Most of chemical reactions consist of the breakage of old bonds and the formation of new ones. The bond with the weakest

dissociation energy, where it easily loses electrons and can be attacked by high-reactive species [20], is the primary breakage position of one molecule according to the bond dissociation energies (BDEs) theory. However, in a real situation the degradation mechanism is hard to be determined due to two reasons. Firstly, the hydroxyl radical is a nonselective and unstable species with an oxidation potential of 2.33 V, which means the oxidation process might be random although the bond with weak dissociation energy is easier to break. For example, the bond energy of C–C, C–N, and C–Cl is 332 kJ·mol⁻¹, 305 kJ·mol⁻¹, and 328 kJ·mol⁻¹, respectively [39]. Among the three bonds, the weakest bond is the C–N bond with the bond energy of 305 kJ·mol⁻¹, which might implicate that the C–N bond would be dissociated first than others based on the BDE theory. However, the chemical component with a molecular formula of C₁₅H₂₀N₂O₅ appears in the intermediate products, which mean the Cl element is dissociated with the C–N bond still containing in the chemical structure. Information on chemical species detected and identified by LC-MS shown in figure 10 is listed in table 2. Secondly, the solution circumstances change with the plasma treatment time, e.g. the chemical components and the solution pH which will influence the chemical activity of some species like the ozone and hydroxyl radical [40–42].

Based on the information on the intermediate products listed in table 2 and BDE theory, the proximate plasma degradation pathways for oxadiazon solution are assumed and presented in figure 11. The oxadiazon molecule is attacked by active species like the hydroxyl radical and ozone in two pathways leading to the formation of D1 and D2 which is detected and confirmed by the presence of m/z peaks at 308.14 and 251.01 respectively. In the first pathway, the formation of D1 during the degradation of oxadiazon solution occurred by dissociating chlorine atoms. The result is qualitatively consistent with the previous reports [23]. In their work, intermediate photochemical transformations of

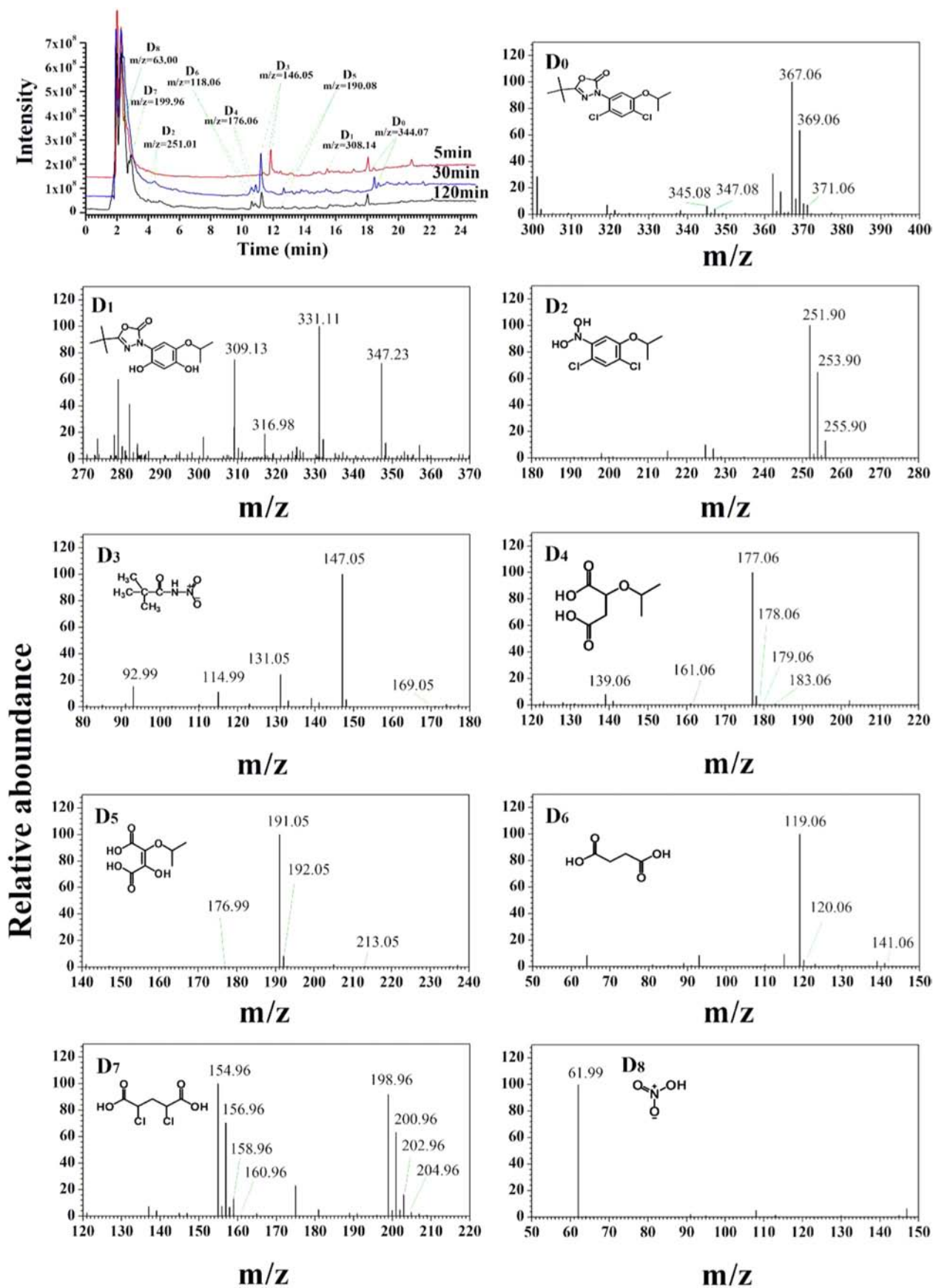
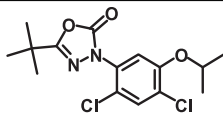
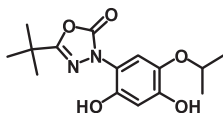
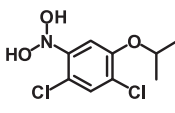
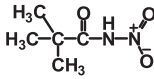
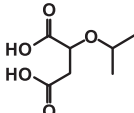
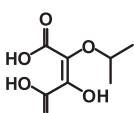
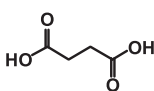
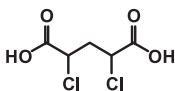
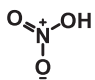


Figure 10. LC-MS spectra of major species in the DBD plasma treated solution.

Table 2. Information on the chemical species observed by LC-MS.

No.	Retention Time (min)	m/z	Observations	
			Molecular Formula	Structural Formula
D ₀	18.77	344.07	C ₁₅ H ₁₈ Cl ₂ N ₂ O ₃	
D ₁	15.79	308.14	C ₁₅ H ₂₀ N ₂ O ₅	
D ₂	3.91	251.01	C ₉ H ₁₁ Cl ₂ NO ₃	
D ₃	11.06	146.07	C ₄ H ₁₀ N ₂ O ₃	
D ₄	10.91	176.07	C ₄ H ₆ Cl ₂ O ₃	
D ₅	12.95	190.05	C ₇ H ₁₀ O ₆	
D ₆	10.43	118.03	C ₄ H ₆ O ₄	
D ₇	2.80	199.96	C ₅ H ₆ Cl ₂ O ₄	
D ₈	2.25	63	HNO ₃	

oxadiazon were dominated by the loss of chlorine atoms and the participation of hydroxyl. The difference occurs in the number of dissociated chlorine atoms. Only single chlorine atom in Ying's report is dissociated from oxadiazon molecular, but there are two chlorine atoms in our work. The reason might rely on the concentration of the generated hydroxyl radicals. In the process presented in this paper, the concentration of the hydroxyl radical, which is denser than the one generated by sunlight, allows the dissociation of both chlorine atoms from oxadiazon molecule. As the degradation process could be developed step by step, it is worth mentioning that the dissociation of one chlorine atom might occur during the degradation. The other pathway leading to the formation of D₂ is mainly confirmed by the chemical species detected and identified by LC-MS. The m/z peak appears at 251.01. Built on the mass spectrum, one nitrogen atom, two chlorine atoms, and nine carbon atoms can be

identified according to the isotope principles and azo principles of mass spectrometry as well as the original chemical structure of oxadiazon [23, 43].

Following the first pathway, the component D₁ performs the ring cleavage as well as the nitrogen removal process, and is further oxidized in two pathways leading to the formation of D₃, D₄, and D₅ which is detected and confirmed by the presence of m/z peaks at 146.07, 176.07, and 190.05 respectively. With further oxidation by hydroxyl radical the component of D₃ performs the nitrogen removal process and transforms into carbon dioxide, water, and D₈ (nitric acid). And the components D₄ and D₅ convert to the component D₆, a kind of micromolecule organic acid, which is detected and confirmed by the presence of m/z peaks at 118.03. Along the pathway, the component D₆ is further oxidized by hydroxyl radical and transformed into carbon dioxide, water. Following the second pathway, the component D₂ undergoes

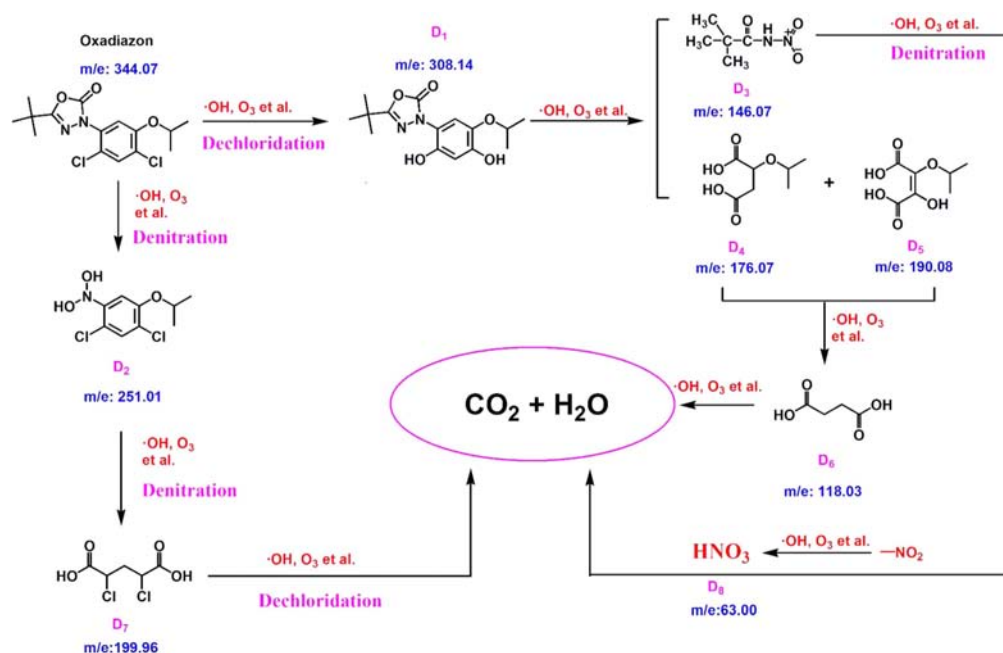


Figure 11. Degradation pathways of oxadiazon by non-thermal plasma.

the ring cleavage process directly, and converts to D7 which is detected and confirmed by the presence of m/z peaks at 199.96, and nitric acid. Then, the component D7 performs a dechlorination process and transforms into carbon dioxide and water. To sum up, the oxadiazon intermediates in solution during plasma degradation are regarded as being formed through dechlorination, denitrification and ring cleavage. The final products are chloride, nitrate, carbon dioxide and water.

It is well known that the electric conductivity relates with the ions dissolved in a solution which can move freely, such as chloridion, nitrate ion, and some organic micromolecule acid generated during the plasma degradation processes, e.g. D4, D5, and D6. As shown in figure 9, the rapid increase of the EC25 attributes to the generation of the chloridion, nitrate ion, and some organic micromolecule acid. Meanwhile, organic micromolecule acid is oxidized into carbon dioxide and water. When the generation of chloridion, nitrate ion, and micromolecule organic acid equals to the loss of organic acid, the EC25 reaches its climax. Then the EC25 decreases with the further loss of the organic acid. Because the generation of chloridion and nitrate ion will be stably dissolved in the solution, the EC25 will be larger than the original one. Depending to this, the results shown in figure 9 are qualitatively consistent with the degradation pathways shown in figure 11. Therefore, it demonstrates further the feasibility and validity of the degradation pathways of oxadiazon by non-thermal plasma.

3.3. The effect of various parameters on COD

As mentioned previously, COD is a measure of the total quantity of oxygen required to oxidize all organic material into carbon dioxide and water. To macroscopically describe the degradation process after plasma treatment, the effect of

various parameters such as applied voltage, solution flow rate, the oxygen flow rate, solution pH, and initial oxadiazon concentration, on the COD and corresponding COD degradation rate is presented.

The role of the plasma degradation attributes to the chemical reactive species, e.g. ozone, hydrogen peroxide, atomic oxygen, hydroxyl radical, which are significantly affected by external electric field intensity. It is common knowledge that some reactive species such as ozone will increase with the electric field intensity, which implies that increasing the applied voltage benefits the degradation process. It is worthy of being noted that the COD from methanol was subtracted for the initial COD of prepared samples. As to the COD from methanol for plasma treated samples, the COD from methanol was assumed to be negligible because of the small amount of methanol (0.009 mL methanol in 60 mL solution). Figure 12(a) presents the variation of COD and degradation rate for plasma treatment time with applied voltage of 4 kV, 5 kV, 6 kV, and 7.5 kV. After 300 min plasma treatment, the COD of the solution sample degrades from about $45\,800\text{ mg}\cdot\text{L}^{-1}$ to about $8901\text{ mg}\cdot\text{L}^{-1}$, $3954\text{ mg}\cdot\text{L}^{-1}$, $2359\text{ mg}\cdot\text{L}^{-1}$, and $2624\text{ mg}\cdot\text{L}^{-1}$ with the applied voltage of 4 kV, 5 kV, 6 kV, and 7.5 kV, respectively. The corresponding COD degradation rate is 80.6%, 91.37%, 94.8%, and 94.3%. As can be observed, the degradation process is greatly improved when the applied voltage increases from 4 kV to 6 kV. However, it is slightly changed when the voltage increases further from 6 kV to 7.5 kV. The reason might be confident that the applied voltage also affects the working gas temperature of the plasma channels. As the applied voltage increases, the temperature of the working gas and even the solution also increases, which then induces the part decomposition of the active species like the ozone

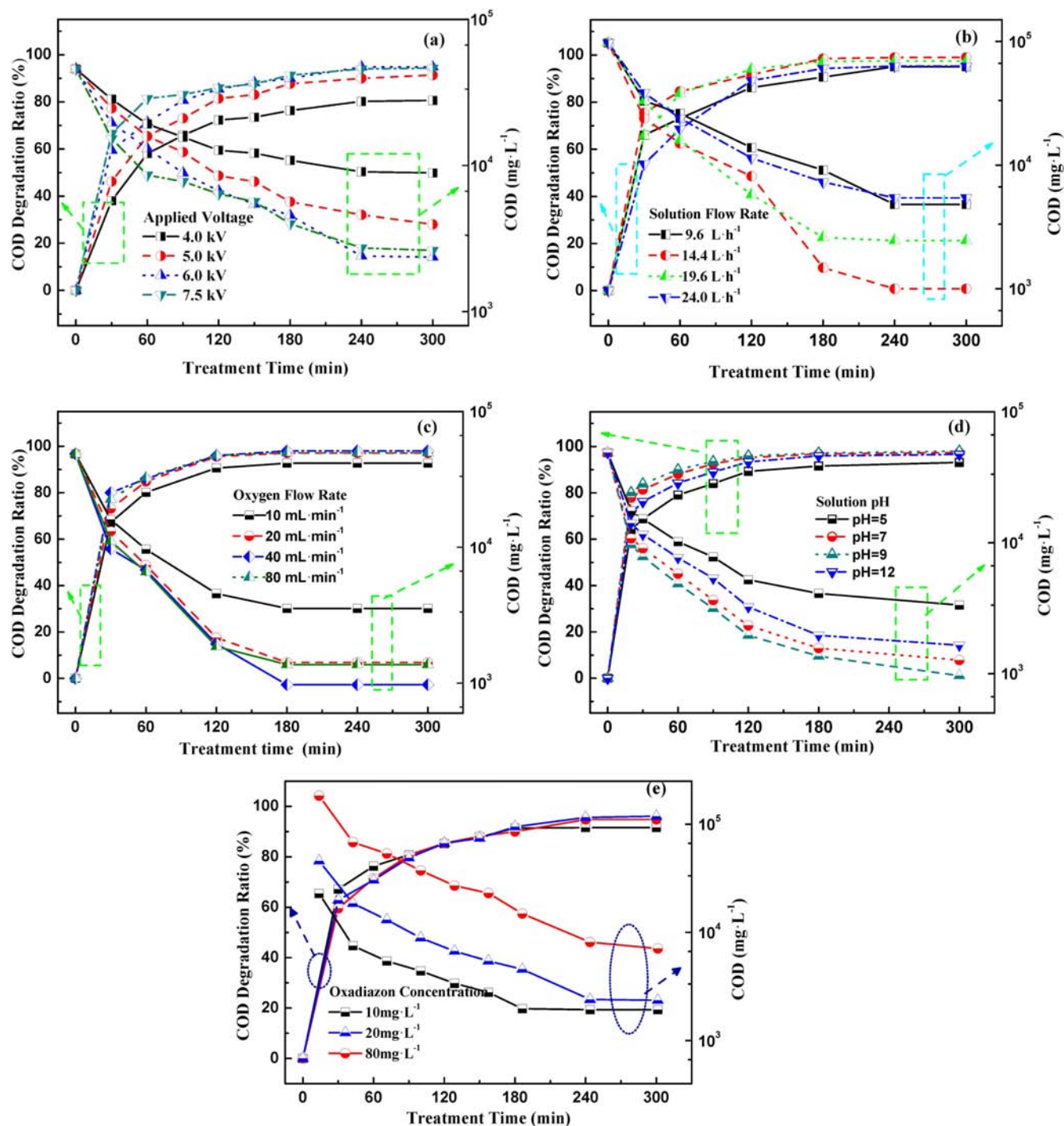


Figure 12. Effects of (a) applied voltage; (b) solution flow rate; (c) oxygen flow rate; (d) solution pH; (e) oxadiazon concentration on COD and degradation ratio.

formed in the plasma channel [16]. Therefore, the degradation process becomes slow.

When the working gas and solution were introduced into the plasma chamber, organics containing on the surface of the solution film was decomposed and degraded by contacting with the chemical active species. Therefore, solution film thickness influences the degradation processes by changing the cycling frequency of the solution, the contacting area with the active species, the discharge intensity, and the contacting time with the active species for one circulation. The

degradation is enhanced by up-regulation of former three factors, but had a negative correlation with the contacting time. The thickness of the solution film can be calculated from the equation $\delta = \frac{Q}{2\pi r\nu}$, where the symbols δ , Q , r , and ν represent the film thickness, solution flow rate, outer diameter of electrode, and the velocity of the water film. It is worth mentioning that the parameter ν is hard to be determined due to the properties of the fluids and the influence of gravity. However, we can still assume the proportional

relation between the film thickness and the solution flow rate. As can be seen in figure 12(b), the COD of the solution sample degrades from about $97\,280\text{ mg}\cdot\text{L}^{-1}$ to about $4800\text{ mg}\cdot\text{L}^{-1}$, $1000\text{ mg}\cdot\text{L}^{-1}$, $2450\text{ mg}\cdot\text{L}^{-1}$, and $5436\text{ mg}\cdot\text{L}^{-1}$ after 300 min plasma treatment with the solution flow rate of $9.6\text{ L}\cdot\text{h}^{-1}$, $14.4\text{ L}\cdot\text{h}^{-1}$, $19.6\text{ L}\cdot\text{h}^{-1}$, and $24.0\text{ L}\cdot\text{h}^{-1}$, respectively. The corresponding COD degradation rate is 95.07%, 98.97%, 97.48%, and 95.3%. It shows that the degradation process is greatly improved when the solution flow rate increases from $9.6\text{ L}\cdot\text{h}^{-1}$ to $14.4\text{ L}\cdot\text{h}^{-1}$. However, it turns to a drop when the flow rate increases further from $14.4\text{ L}\cdot\text{h}^{-1}$ to $24.0\text{ L}\cdot\text{h}^{-1}$. As mentioned previously, the increase of solution film thickness influence the degradation processes by increasing the cycling frequency of the solution, the contacting area with the active species, discharge intensity, and the contacting time with the active species for one circulation. Although the enhanced solution flow rate increases the cycling frequency and slightly increases the contacting area with the active species, the contacting and reacting time decrease because the degradation progress mainly occurs on the contacting surface. The positive aspects are dominant when the solution flow rate is increasing from $9.6\text{ L}\cdot\text{h}^{-1}$ to $14.4\text{ L}\cdot\text{h}^{-1}$. However, the negative aspects play a dominant role when the flow rate increases from $14.4\text{ L}\cdot\text{h}^{-1}$ to $24.0\text{ L}\cdot\text{h}^{-1}$.

Figure 12(c) shows the variation of COD and degradation rate for plasma treatment time with an oxygen flow rate of $10\text{ mL}\cdot\text{min}^{-1}$, $20\text{ mL}\cdot\text{min}^{-1}$, $40\text{ mL}\cdot\text{min}^{-1}$, and $80\text{ mL}\cdot\text{min}^{-1}$. The COD of the solution sample degrades from about $48\,640\text{ mg}\cdot\text{L}^{-1}$ to about $3548\text{ mg}\cdot\text{L}^{-1}$, $1420\text{ mg}\cdot\text{L}^{-1}$, $972.8\text{ mg}\cdot\text{L}^{-1}$, and $1370\text{ mg}\cdot\text{L}^{-1}$ after 180 min plasma treatment with the oxygen flow rate of $10\text{ mL}\cdot\text{min}^{-1}$, $20\text{ mL}\cdot\text{min}^{-1}$, $40\text{ mL}\cdot\text{min}^{-1}$, and $80\text{ mL}\cdot\text{min}^{-1}$, respectively. Accordingly, the COD degradation rate is 92.71%, 97.08%, 98%, and 97.18%. As can be observed, the degradation process is greatly improved when the oxygen flow rate increases from $10\text{ mL}\cdot\text{min}^{-1}$ to $40\text{ mL}\cdot\text{min}^{-1}$. However, it is slightly changed when the flow rate increases further from $40\text{ mL}\cdot\text{min}^{-1}$ to $80\text{ mL}\cdot\text{min}^{-1}$. It is known that increasing the oxygen concentration will increase the concentration of the strong oxidizing species like ozone. Meanwhile, the increase of the oxygen concentration will reduce the plasma discharge intensity by adsorbing electrons due to its strong electronegativity. Therefore, the effect of oxygen flow rate on the degradation process depends on that which aspect plays the dominant role.

As it is known, the reaction rate constant in aqueous solution depends on the reactant concentration and the surrounding circumstances like temperature and solution pH. Generally, the alkaline environment contributes to the oxidation reaction, while the acidic condition benefits from the reduction reaction. From this viewpoint, the increase of solution pH is beneficial to the oxadiazon degradation [40, 44]. Figure 12(d) shows the variation of COD and degradation rate with plasma treatment time with solution pH of 5, 7, 9, and 12. The COD of the solution sample degrades from about $48\,640\text{ mg}\cdot\text{L}^{-1}$ to about $3340\text{ mg}\cdot\text{L}^{-1}$, $1268\text{ mg}\cdot\text{L}^{-1}$, $964\text{ mg}\cdot\text{L}^{-1}$, and $1648\text{ mg}\cdot\text{L}^{-1}$ after 300 min

plasma treatment with the solution pH of 5, 7, 9, and 12, respectively. Accordingly, the COD degradation rates are 93.13%, 97.39%, 98.02%, and 96.61%. As can be observed, the degradation process is greatly improved when the solution pH increases from 5 to 9. However, it gets worse when the solution pH increases further from 9 to 12. It seems contradictory to the previous thesis that the alkaline environment contributes to the oxidation reaction. The potential reason for this phenomenon is that the solution pH changes the chemical composition of the ozone; for instance OH radicals were formed by decomposing ozone at high pH, whereas the molecular ozone content remained unchanged at a low pH. Moreover, the oxidation potentials of the reactive species are strongly influenced by solution pH. The oxidizing potential of hydroxyl radical drops from 2.7 V at pH = 3 to 2.34 V at pH = 9 [41], and the oxidizing potential of ozone decreases from 2.08 V at acidic pH to 1.4 V in alkaline condition [40]. In addition, ozone exists as molecular in an acidic environment, but its stability declined with increasing pH, resulting in generation of short-lived oxidants radicals such as OH, HO₂, HO₃ and HO₄ under alkaline conditions [42]. And, therefore, the effect of solution pH on the oxadiazon degradation process mainly depends on the combined interactions of such factors mentioned previously.

Figure 12(e) shows the variation of COD and degradation rate for plasma treatment time with initial oxadiazon concentration of $10\text{ mg}\cdot\text{L}^{-1}$, $20\text{ mg}\cdot\text{L}^{-1}$, and $80\text{ mg}\cdot\text{L}^{-1}$. For the solution sample with initial concentration of $10\text{ mg}\cdot\text{L}^{-1}$, $20\text{ mg}\cdot\text{L}^{-1}$, and $80\text{ mg}\cdot\text{L}^{-1}$, the initial COD are $23\,916\text{ mg}\cdot\text{L}^{-1}$, $45\,800\text{ mg}\cdot\text{L}^{-1}$, and $181\,620\text{ mg}\cdot\text{L}^{-1}$, respectively. After 300 min plasma treatment, they degrade to about $1925\text{ mg}\cdot\text{L}^{-1}$, $2359\text{ mg}\cdot\text{L}^{-1}$, and $7080\text{ mg}\cdot\text{L}^{-1}$, respectively. Accordingly, the COD degradation rate is about 91.59%, 94.8%, and 96.1%. As can be observed, COD after plasma treatment increases with oxadiazon concentration despite the fact the degradation rate is increasing.

4. Conclusion

In this paper, degradation of the oxadiazon in solution by non-thermal plasma with a dielectric barrier configuration was investigated. The effect of various parameters such as applied voltage, solution flow rate, the oxygen flow rate, solution pH, and initial oxadiazon concentration, on the COD and corresponding COD degradation rate is presented. The effect of initial oxadiazon on COD and COD degradation presented inconsistently. The COD as well as the degradation rate after plasma treatment increases with oxadiazon concentration. The HPLC results indicate the rapid removal of oxadiazon in solution, and the possible change rule of the intermediate products during the plasma degradation. The TOC detection shows the continuous decrease with the plasma degradation process, which indicates that the carbon element containing in oxadiazon is transformed gradually into carbon dioxide. According to the OES and LC-MS analysis, possible degradation pathways are proposed. The non-thermal plasma degradation pathways of oxadiazon in solution involved the

loss of the nitro group, dechlorination and ring cleavage. There are two pathways leading to separate degradation processes, i.e. the priority of the dissociation of chlorine atoms to the nitrogen atoms, and the priority of the dissociation of nitrogen atoms to the chlorine atoms. The first pathway is qualitatively consistent with the previous reports. The detection of EC25 and the productions of chloridion and nitrate ion demonstrates further the feasibility and validity of the non-thermal plasma degradation pathways of oxadiazon. The final products are chloride, nitrate, carbon dioxide and water after the non-thermal plasma treatment.

Acknowledgments

The authors would like to thank Dr Hao Yin, Dr Shuai Gong, and Dr Airong Feng at University of Science and Technology of China for their valuable assistance with the LC-MS detection and analysis, and Dr Kuilin Wang for his kind help improving the English. This work is supported financially by the National Natural Science Foundation of China under Grant Nos. 11205201, 11575252, and 11575253.

References

- [1] WHO/UNICEF Joint Monitoring Programme 2000 *Global Water Supply and Sanitation Assessment 2000 Report* (New York: World Health Organization)
- [2] Tijani J O et al 2014 *Water Air Soil Pollut.* **225** 2102
- [3] Chakraborty S K, Bhattacharya A and Chowdhury A 1999 *Pesticide Science* **55** 943
- [4] Chakraborty S K et al 1995 *J. Agric. Food. Chem.* **43** 2964
- [5] Gomez J et al 1982 *J. Agric. Food. Chem.* **30** 772
- [6] Comoretto L et al 2008 *Environ. Pollut.* **151** 486
- [7] Staehelin J and Hoigne J 1985 *Environ. Sci. Technol.* **19** 1206
- [8] Patil A L, Patil P N and Gogate P R 2014 *Ultrasonics Sonochem.* **21** 1778
- [9] Vilhunen S and Sillanpaa M 2010 *Rev. Environ. Sci. Biotechnol.* **9** 323
- [10] Vilhunen S et al 2010 *J. Hazard Mater.* **1-3** 776
- [11] Poupopoulos S G, Arvanitakis F and Philippopoulos C J 2006 *J. Hazard. Mater.* **129** 64
- [12] Vilve M et al 2010 *Environ. Sci. Pollut. Res.* **17** 875
- [13] Arana J et al 2008 *Chemosphere* **71** 788
- [14] Horikoshi S, Hidaka H and Serpone N 2002 *Environ. Sci. Technol.* **36** 5229
- [15] Vescovi T, Coleman H M and Amal R 2010 *J. Hazard. Mater.* **182** 75
- [16] Zhang R et al 2007 *J. Hazard. Mater.* **142** 105
- [17] Stara Z et al 2009 *Desalination* **239** 283
- [18] Busca G et al 2008 *J. Hazard. Mater.* **160** 265
- [19] Sun B, Sato M and Clements J S 2000 *Environ. Sci. Technol.* **34** 509
- [20] Xue J, Chen L and Wang H 2008 *Chem. Eng. J.* **138** 120
- [21] Magureanu M et al 2008 *J. Appl. Phys.* **104** 103306
- [22] Klavarioti M, Mantzavinos D and Kassinos D 2009 *Environ. Int.* **35** 402
- [23] Ying G and Williams B 1999 *J. Environ. Sci. Health B* **34** 549
- [24] Al-Mutlaq K F 2006 *Environ. Geol.* **51** 493
- [25] Garbi C et al 2006 *Water Res.* **40** 1217
- [26] Pinilla P et al 2008 *Bioresource Technol.* **99** 2177
- [27] Ying G G and Williams B 2000 *Environ. Pollut.* **107** 399
- [28] Mokhlesur R M and Jang-Eok K 2010 *J. Korean Soc. Appl. Biol. Chem.* **53** 458
- [29] Joshi R P and Thagard S M 2013 *Plasma Chem. Plasma Process.* **33** 17
- [30] Shi J, Bian W and Yin X 2009 *J. Hazard. Mater.* **171** 924
- [31] Magureanu M et al 2011 *Water Res.* **45** 3407
- [32] Yanan L et al 2012 *Chem. Eng. Process.* **56** 10
- [33] Kil-Seong K, Churl-Shin Y and Mok Y S 2013 *Chem. Eng. J.* **219** 19
- [34] Maria H-V et al 2013 *Water Res.* **47** 1701
- [35] Chen B Y et al 2014 *Plasma Sci. Technol.* **16** 1126
- [36] Fieser L F and Fieser M 1959 *Steroids* (New York: Reinhold Publishing Corporation) p 15
- [37] Woodward R B 1941 *J. Am. Chem. Soc.* **63** 1123
- [38] Woodward R B 1942 *J. Am. Chem. Soc.* **64** 76
- [39] Luo Y R 2005 *Handbook of Bond Dissociation Energies in Organic Compounds* (Beijing: Science Press)
- [40] Hoigen J and Bader H 1976 *Water Res.* **10** 377
- [41] Gao J Z et al 2004 *Plasma Process Polym.* **1** 171
- [42] Muthukumar M et al 2004 *Dye Pigment* **63** 127
- [43] Silverstein R M et al 2005 *Spectrometric Identification of Organic Compounds* (New York: Wiley)
- [44] Hoigen J and Bader H 1983 *Water Res.* **17** 185